

Electronic supplementary information (ESI)

**Electrochemically shape-controlled synthesis of great stellated
dodecahedral Au nanocrystals with high-index facets for
nitrogen reduction to ammonia**

Yu-Chen Jiang,^a Yu-Jie Mao,^a Jin Zou,^a Hong-Hui Wang,^b Feng Liu,^a Yong-Sheng Wei,^a Tian Sheng,*^c Xin-Sheng Zhao,^a Lu Wei*^a

^a School of Physics and Electronic Engineering, Jiangsu Normal University, Xuzhou 221116, E-mail: lwei057@jsnu.edu.cn

^b School of Environmental Science & Engineering, Xiamen University Tan Kah Kee College, Zhangzhou 363105, China.

^c College of Chemistry and Materials Science, Anhui Normal University, Wuhu, 241000, China. E-mail: tsheng@ahnu.edu.cn

1. Chemical and materials

Hydrogen tetrachloroaurate trihydrate ($\text{HAuCl}_4 \cdot 3\text{H}_2\text{O}$, 99.9%), choline chloride ($\text{HOCH}_2\text{CH}_2\text{N}(\text{CH}_3)_3\text{Cl}$, 99%), urea ($\text{CO}(\text{NH}_2)_2$, AR reagent, >99%), hydrochloric acid (HCl, AR reagent, 36.0~38.0%), perchloric acid (HClO_4 , GR reagent), sulfuric acid (H_2SO_4 , GR reagent, 95~98%), sodium hydroxide (NaOH, AR reagent), salicylic acid (AR reagent), sodium citrate (AR reagent), sodium hypochlorite aqueous solution (NaClO , AR reagent), sodium nitroferricyanide ($\text{C}_5\text{FeN}_6\text{Na}_2\text{O}$, AR reagent), para-(dimethylamino) benzaldehyde (AR reagent) and Au spheres (CAS: 7440-57-5, 0.5~0.8 μm) were purchased from Sinopharm Chemical Reagent Co. Ltd (Shanghai, China).

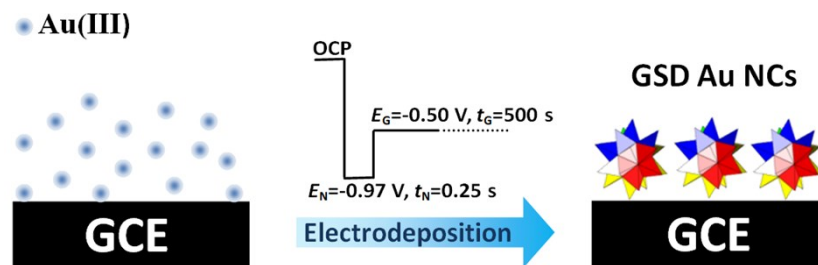
2. Preparation of deep eutectic solvent

The typical preparation of choline chloride-urea (ChCl-U) based deep eutectic solvent (DES) was described in detail in previous reports.^{S1-S3} In short, purified ChCl and urea were mixed in a beaker at a defined ratio (ChCl: urea = 1: 2, molar ratio) and stirred at 80 °C until a uniform colorless liquid formed. The as-prepared DES was then stored in a vacuum of 80 °C before use.

3. Synthesis of great stellated dodecahedral Au nanocrystals

The GSD Au nanocrystals (NCs) were synthesized by electrodeposition in a standard three-electrode cell connected to a CHI 760E electrochemical workstation (Shanghai Chenhua Instrumental Co., Ltd., China), with a platinum wire counter

electrode and a platinum quasi-reference electrode. The working electrode was a glassy carbon disk (GC, $\Phi = 6$ mm). Prior to each electrodeposition, the GC was polished using a fine mechanical Al_2O_3 with powder size of 1.0 and 0.3 μm and then cleaned ultrasonically in an ultrapure water bath. In a typical synthesis, the GSD Au NCs were synthesized by a double-step potential method in an ageing ChCl-urea based DES solution containing 24.28 mM HAuCl_4 at 60 °C. The ageing time of HAuCl_4 /DES solution is more than 5 months and the ageing temperature is 28 °C. In detail, the GC working electrode was first subjected at open circuit potential (OCP), soon afterwards step to nucleation potential (E_N) of -0.97 V (vs. Pt) for 0.25 s, then step to growth potential (E_G) of -0.50 V for 500 s, as shown in Scheme S1.



Scheme S1. Illustration of the electrodeposition procedure for preparation of GSD Au NCs.

4. ICP-MS Analysis

The inductively coupled plasma mass spectrometry method (ICP-MS) was carried out to quantify the amount of Au on the as-prepared GSD Au NCs electrode, as listed in Table S1. The result shows that the Au loading on the as-prepared GSD Au NCs electrode is 9.18 μg .

Table S1. ICP-MS results of Au on the as-prepared GSD Au NCs electrodes.

Samples	Content / μg	Average value / μg
1#	9.425	9.18
2#	9.325	
3#	8.800	

5. Preparation of working electrode using commercial Au spheres catalyst

To prepare the working electrode, 3.0 mg of the Au spheres (CAS: 7440-57-5, 0.5~0.8 μm) and 100 μL Nafion alcohol solution (5 wt %) were dispersed into 3 mL ultrapure water under ultrasonic treatment for 10 min. Then 10 μL of the treated Au spheres ink was transferred onto a glassy carbon (GC, $\Phi = 6 \text{ mm}$) electrode and dried in air, denoted as Au spheres/GC electrode. The Au loading on the as-prepared commercial Au spheres catalyst electrode is 10 μg . Prior to preparation, the GC electrode was polished mechanically by using finer Al_2O_3 powder with sizes of 1.0 μm and then cleaned ultrasonically in an ultrapure water bath.

6. Structure characterization

Scanning electron microscopy (SEM) images of great stellated dodecahedral Au NCs were analyzed using SU8010 electron microscope. Transmission electron microscopy (TEM) measurements were carried out on a FEI Tecnai-F30 electron microscope with an operating voltage of 300 kV. HAADF imaging and mappings

were executed using a JEOL ARM200F (JEOL, Tokyo, Japan) STEM with an accelerating voltage of 200 kV with a thermal field-emission gun and a probe Cs corrector (CEOS GmbH, Heidelberg, Germany).

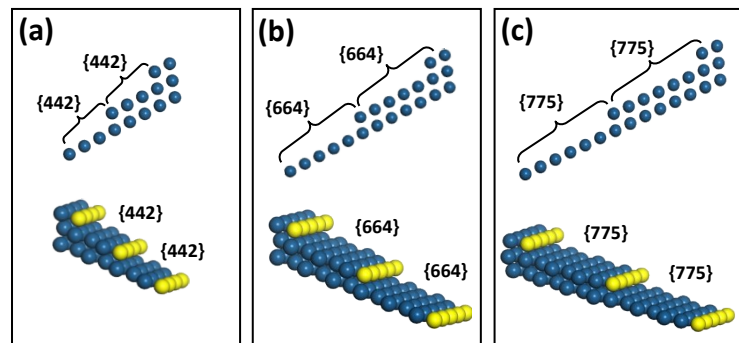


Fig. S1 Atomic models of (a) Au{442}, (b) Au{664} and (c) Au{775} planes, respectively.

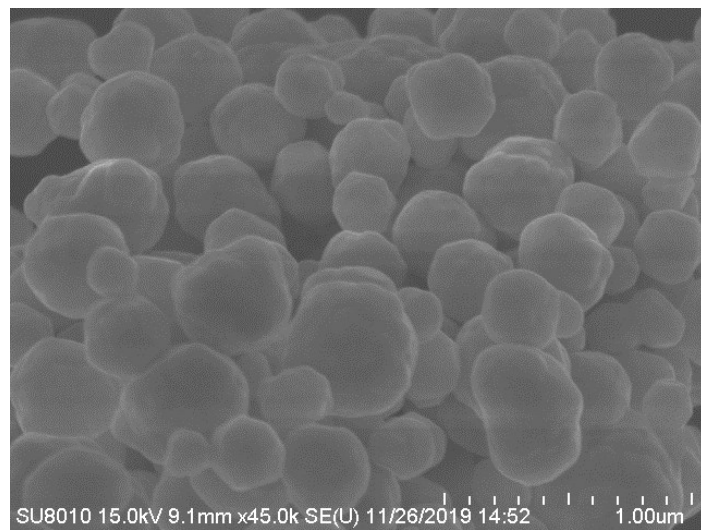


Fig. S2 SEM image of Au spheres (CAS: 7440-57-5, 0.5~0.8 μm) purchased from Alfa Aesar Co. Ltd.

7. Electrochemical characterization

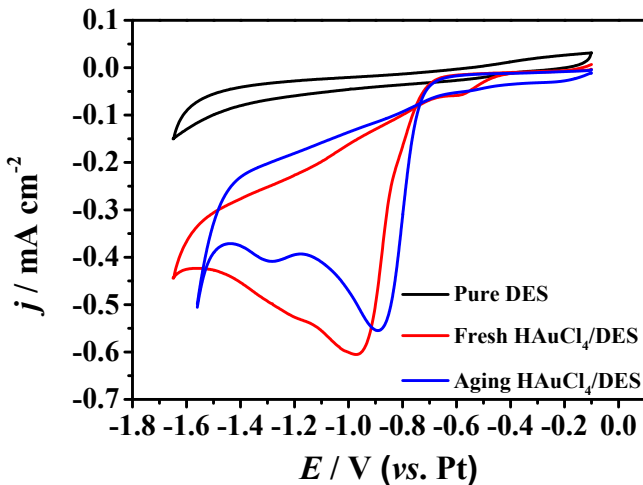


Fig. S3 Cyclic voltammograms recorded on GC electrode in pure DES, fresh and aging HAuCl₄/DES solutions.

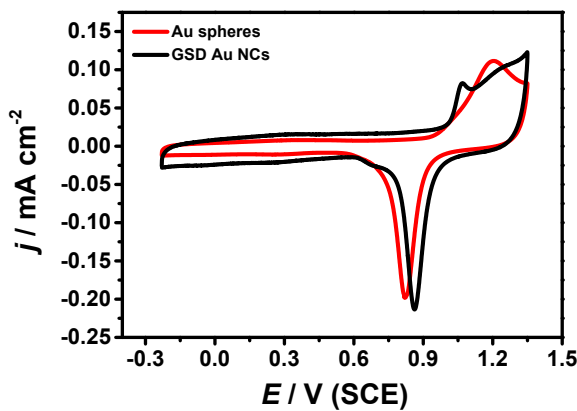


Fig. S4 Cyclic voltammograms recorded on the GSD Au NCs and Au spheres in 0.1 M HClO₄ solution. Scan rate: 50 mV s⁻¹; temperature: 25°C.

The electrochemical characterization of the GSD Au NCs was carried out in 0.1 M HClO₄ solution at room temperature (25 °C). The solution was deaerated by

purging with pure N₂ gas before experiment, and a flux of N₂ was kept over the solution during measurements to prevent the interference of atmospheric oxygen. A saturated calomel electrode (SCE) was used as reference electrode.

8. Electrocatalytic nitrogen reduction measurements

The NRR activity tests were conducted in a standard three-electrode cell containing 30 mL of 1 mM HCl solution under ambient conditions, in which the cathode and anode was separated by the Nafion-211 membrane. Before NRR test, the Nafion 211 membrane was heated in 5 % H₂O₂, 0.5 M H₂SO₄, and ultrapure water at 80 °C for 1 h, respectively. A graphite flake electrode and a saturated calomel electrode (SCE) were used as the counter and reference electrodes, respectively. For electrochemical N₂ reduction, chronoamperometry tests were carried out at different potentials in N₂-saturated 1 mM HCl solution, which was purged with N₂ for 1 hr before the measurement. The NRR products were spectrophotometrically determined by the indophenol indicator and the Watt and Chrisp methods.^{30,31} The calibration curve for the NH₃ meter is shown in Fig. S5. The NH₃ yield rate (*r*) and Faradaic efficiency (FE) are calculated by the following equations:

$$r(NH_3) = \frac{[NH_3] \times V}{t \times A} \quad (1)$$

$$FE(NH_3) = \frac{Q_{NH_3}}{Q_{total}} \frac{3 \times 96500 \times [NH_3] \times V}{\int idt} \quad (2)$$

Where *A* is the electrochemically active surface area, which was calculated using the charge associated with the reduction of a full monolayer of Au oxides (Fig. S4).

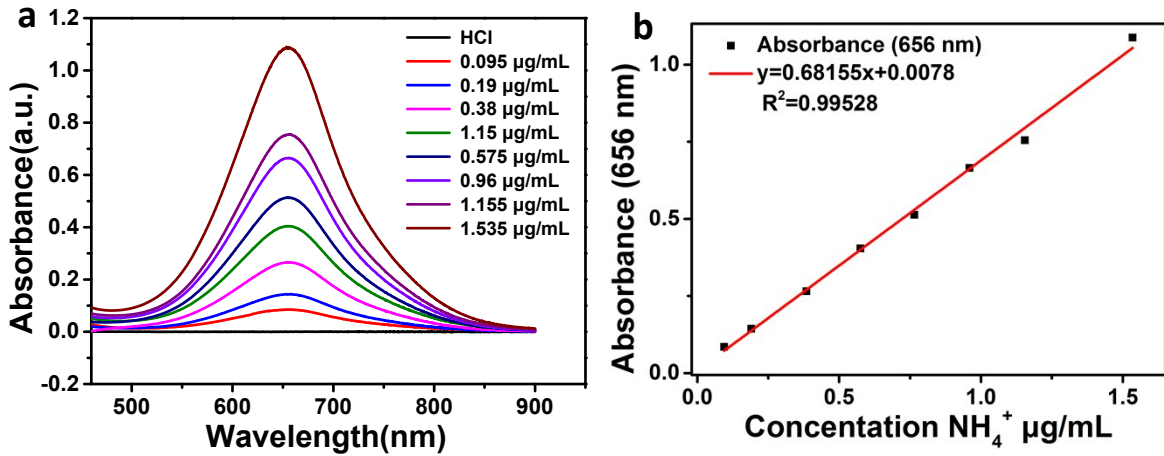


Fig. S5 Absolute calibration of the indophenol blue method using ammonium chloride solutions of known concentration as standards. (a) UV-Vis curves of indophenol assays with NH_4^+ ions after incubated for 1 hour at room temperature; (b) calibration curve used for estimation of NH_3 by NH_4^+ ion concentration. The absorbance at 656 nm was measured by UV-Vis spectrophotometer, and the fitting curve shows good linear relation of absorbance with NH_4^+ ion concentration ($y = 0.6815x + 0.0078$, $R^2 = 0.99528$) of three times independent calibration curves.

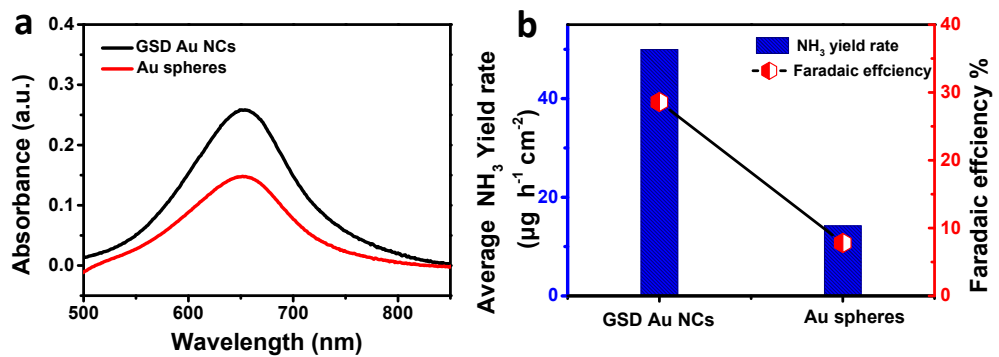


Fig. S6 (a) UV-vis absorption spectra of the electrolytes stained with an indophenol blue indicator after NRR electrolysis at -0.4 V on the GSD Au NCs and Au spheres. (b) Yield rate of NH_3 and Faradaic efficiency at -0.4 V on the GSD Au NCs and Au spheres.

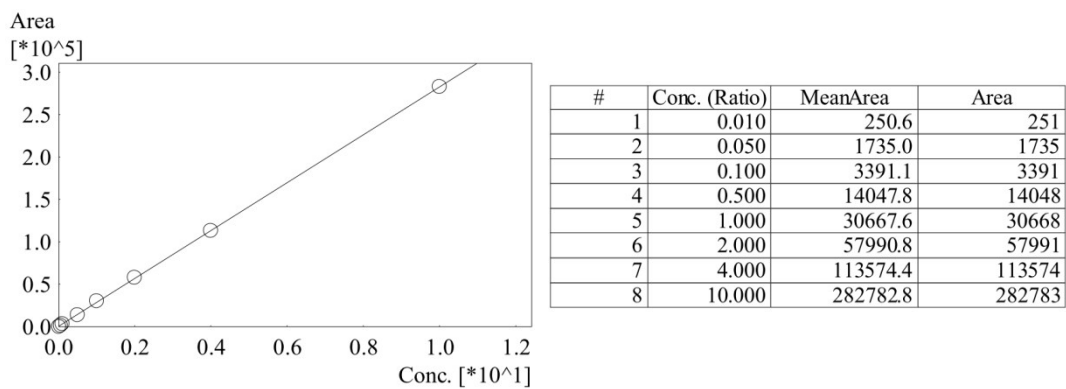


Fig. S7 calibration curve used for estimation of NH_4^+ ion concentration by ion chromatography

method.

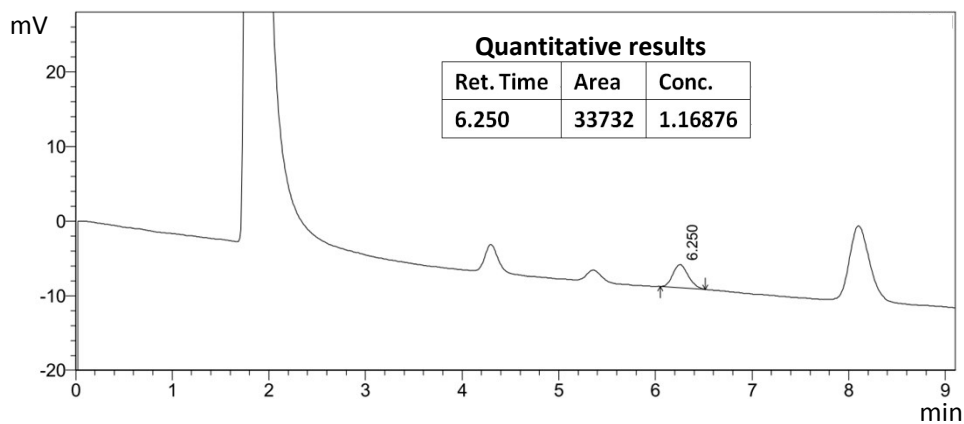


Fig. S8 Ion chromatography of the electrolytes after NRR electrolysis on the GSD Au NCs at -0.4 V (vs. RHE) for 2 h.

9. Durability tests

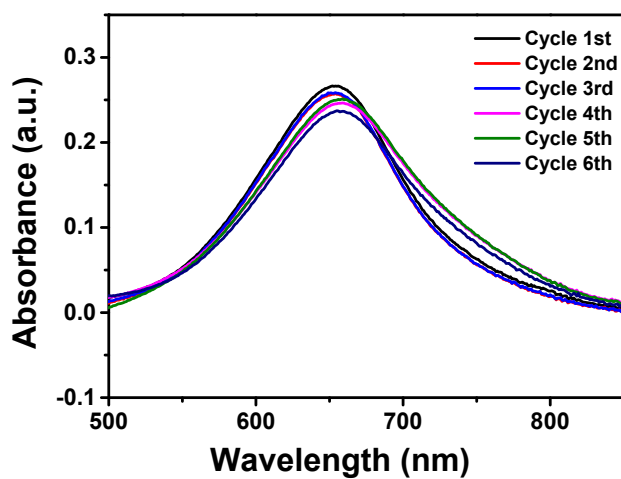


Fig. S9 UV-Vis absorption spectra of the electrolytes stained with indophenol blue indicator after NRR electrolysis on the GSD Au NCs in 1 mM HCl solution for different cycling tests.

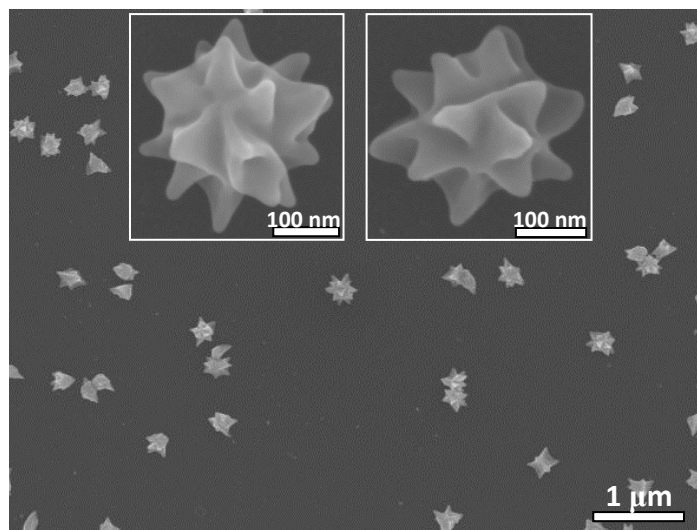


Fig. S10 SEM image of the GSD Au NCs obtained after NRR endurance cycle test, confirming that the Au NCs still kept the GSD shape after the reaction. The insets show the high-magnification SEM images.

10. Determination of N₂H₄

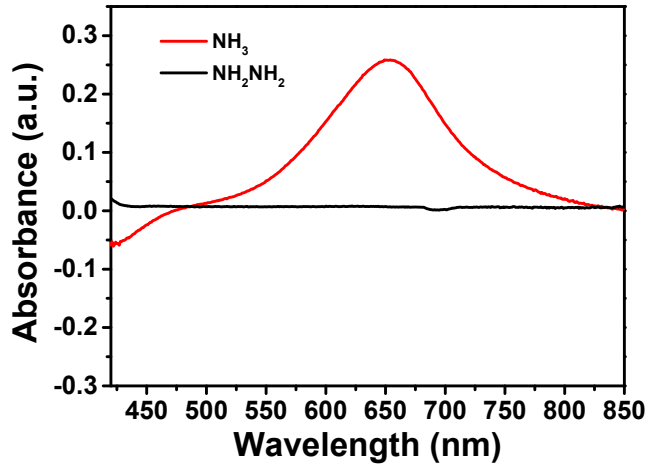


Fig. S11 UV-vis absorption spectra of the electrolytes stained with indophenol blue indicator (red line) and Watt-Chrisp (black line) methods after NRR electrolysis on GSD Au NCs at -0.4 V for 2 h.

11. Isotope labelling experiments

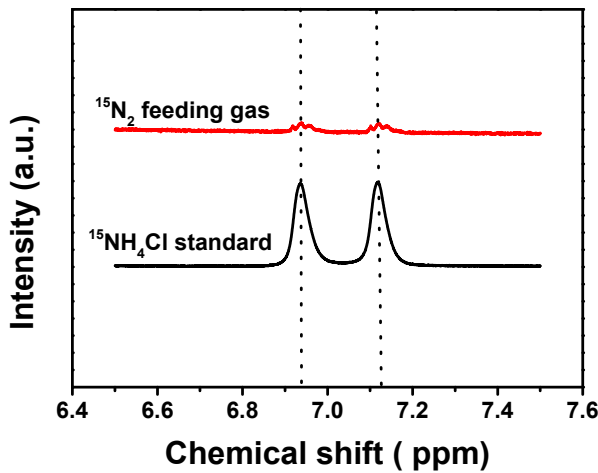


Fig. S12 ¹H NMR spectra of the electrolyte after the NRR test at -0.4 V using ¹⁵N₂ as the feed gas in 1 mM HCl and ¹⁵NH₄Cl standard.

12. Summary of the representative reports on NRR electrocatalysts

Table S2 Summary of the representative reports on NRR electrocatalysts under ambient conditions.

Electrocatalysts	Electrolytes	r_{NH_3}	FE (%)	Overpotential(V/RHE)	Ref.
GSD Au NCs	1 mM HCl	49.96 $\mu\text{g h}^{-1} \text{cm}^{-2}$	28.59	-0.4	This work
a-Au/CeO _x -RGO	0.1 M HCl	8.3 $\mu\text{g h}^{-1} \text{mg}^{-1}_{\text{cat}}$	10.10	-0.2	5
Au THH NR	0.1 M KOH	1.648 $\mu\text{g h}^{-1} \text{cm}^{-2}$	4.0	-0.2	23
pAu/NF	0.1 M Na ₂ SO ₄	9.42 $\mu\text{g h}^{-1} \text{cm}^{-2}$	13.36	-0.2	S4
Au SAs-NDPCs	0.1 M HCl	2.32 $\mu\text{g h}^{-1} \text{cm}^{-2}$	12.3	-0.2	S5
Au NPs	0.1 M Li ₂ SO ₄	9.22 $\mu\text{g h}^{-1} \text{cm}^{-2}$	73.32	-0.3	6
Au/Ti ₃ C ₂	0.1 M HCl	30.06 $\mu\text{g h}^{-1} \text{mg}^{-1}_{\text{cat}}$	18.34	-0.2	S6
BD-Ag/AF	0.1 M Na ₂ SO ₄	$2.07 \times 10^{-11} \text{ mol s}^{-1} \text{cm}^{-2}$	7.36	-0.6	S7
Ag nanosheet	0.1 M HCl	$4.62 \times 10^{-11} \text{ mol s}^{-1} \text{cm}^{-2}$	4.8	-0.6	7
Ag TPs	0.1-0.6 M K ₂ SO ₄	58.5 $\text{mg h}^{-1} \text{g}_{\text{Ag}}^{-1}$	25	-0.25	S8
Pd-TA	0.1 M Na ₂ SO ₄	24.12 $\mu\text{g h}^{-1} \text{mg}^{-1}_{\text{cat}}$	9.49	-0.45	8
Ru SAs/g-C ₃ N ₄	0.5 M NaOH	23.0 $\mu\text{g h}^{-1} \text{mg}^{-1}_{\text{cat}}$	8.3	0.05	9
Ru@ZrO ₂ /NC	0.1 M HCl	3.665 $\text{mg h}^{-1} \text{mg}^{-1}_{\text{cat}}$	15	-0.21	10
Ru NPs	0.01 M HCl	5.5 $\text{mg h}^{-1} \text{m}^{-2}$	5.4	-0.1	S9
Dendritic Cu	0.1 M HCl	25.63 $\mu\text{g h}^{-1} \text{mg}^{-1}_{\text{cat}}$	15.12	-0.4	S10
Cu NPs-rGO	0.5 M LiClO ₄	24.58 $\mu\text{g h}^{-1} \text{mg}^{-1}_{\text{cat}}$	15.32	-0.4	S11
Ag-Au nanocages	0.5 M LiClO ₄	3.74 $\mu\text{g h}^{-1} \text{cm}^{-2}$	35.9	-0.4	S12
Au ₁ Cu ₁	0.05 M H ₂ SO ₄	154.91 $\mu\text{g h}^{-1} \text{mg}^{-1}_{\text{cat}}$	54.96	-0.2	S13
AuPdP NWs	0.1 M Na ₂ SO ₄	7.51 $\mu\text{g h}^{-1} \text{cm}^{-2}$	15.44	-0.3	S14
PdAg	1 M KOH	24.1 $\mu\text{g h}^{-1} \text{mg}^{-1}$	1.7	-0.2	S15
Pd ₃ Cu ₁	1 M KOH	39.9 $\mu\text{g h}^{-1} \text{mg}^{-1}_{\text{cat}}$	1.22	-0.25	S16
Pd-Co/CuO	0.1 M KOH	10.04 $\mu\text{g h}^{-1} \text{mg}^{-1}_{\text{cat}}$	2.16	-0.2	S17
PdRu TPs	0.1 M KOH	37.23 $\mu\text{g h}^{-1} \text{mg}^{-1}_{\text{cat}}$	1.85	-0.2	S18
RhCu-BUNNs	0.1 M KOH	95.06 $\mu\text{g h}^{-1} \text{mg}^{-1}_{\text{cat}}$	1.5	-0.2	S19
TiO ₂ nanosheets	0.1 M H ₂ SO ₄	35.6 $\mu\text{g h}^{-1} \text{mg}^{-1}_{\text{cat}}$	5.3	-0.8	S20
d-TiO ₂ /TM	0.1 M HCl	$1.24 \times 10^{-10} \text{ mol s}^{-1} \text{cm}^{-2}$	9.17	-0.15	S21
VO ₂	0.1 M Na ₂ SO ₄	14.85 $\mu\text{g h}^{-1} \text{mg}^{-1}_{\text{cat}}$	3.97	-0.7	S22
Cr ₂ O ₃ -rGO	0.1 M HCl	33.3 $\mu\text{g h}^{-1} \text{mg}^{-1}_{\text{cat}}$	7.33	-0.7	S23
Cr ₂ O ₃ nanofiber	0.1 M HCl	28.13 $\mu\text{g h}^{-1} \text{mg}^{-1}_{\text{cat}}$	8.56	-0.75	11
MnO-CNF	0.1 M Na ₂ SO ₄	35.9 $\mu\text{g h}^{-1} \text{mg}^{-1}_{\text{cat}}$	1.52	-1.25	S24
Mn ₃ O ₄ @rGO	0.1 M Na ₂ SO ₄	17.4 $\mu\text{g h}^{-1} \text{mg}^{-1}_{\text{cat}}$	3.52	-0.85	S25
Mn ₃ O ₄ nanocube	0.1 M Na ₂ SO ₄	11.6 $\mu\text{g h}^{-1} \text{mg}^{-1}_{\text{cat}}$	3.0	-0.8	S26
a-Fe ₂ O ₃	0.1 M KOH	32.13 $\mu\text{g h}^{-1} \text{mg}^{-1}_{\text{cat}}$	6.63	-0.3	12
p-Fe ₂ O ₃ /CC	0.1 M Na ₂ SO ₄	6.78 $\mu\text{g h}^{-1} \text{cm}^{-2}$	7.69	-0.4	S27

Table S2 (continued)

Fe ₂ O ₃ nanorods	0.1 M Na ₂ SO ₄	15.9 µg h ⁻¹ mg ⁻¹ _{cat}	0.94	-0.8	S28
Fe ₃ O ₄ nanorod	0.1 M Na ₂ SO ₄	5.6×10 ⁻¹¹ mol s ⁻¹ cm ⁻²	2.6	-0.4	S28
CoO QD/RGO	0.1 M Na ₂ SO ₄	21.5 µg h ⁻¹ mg ⁻¹	8.3	-0.6	S30
NiO/CC	0.1 M LiClO ₄	22.7 µg h ⁻¹ mg ⁻¹	7.3	-0.5	S31
NiO/G	0.1 M Na ₂ SO ₄	18.6 µg h ⁻¹ mg ⁻¹	7.8	-0.7	S32
CuO/RGO	0.1 M Na ₂ SO ₄	1.8×10 ⁻¹⁰ mol s ⁻¹ cm ⁻²	3.9	-0.75	S33
ZnO/RGO	0.1 M Na ₂ SO ₄	17.7 µg h ⁻¹ mg ⁻¹	6.4	-0.65	S34
Y ₂ O ₃ nanosheet	0.1 M Na ₂ SO ₄	1.06×10 ⁻¹⁰ mol s ⁻¹ cm ⁻²	2.53	-0.9	S35
NbO ₂ NPs	0.05 M H ₂ SO ₄	11.6 µg h ⁻¹ mg ⁻¹ _{cat}	32	-0.65	S36
SnO ₂ /CC	0.1 M Na ₂ SO ₄	1.47×10 ⁻¹⁰ mol s ⁻¹ cm ⁻²	2.17	-0.8	13
SnO ₂ /RGO	0.1 M Na ₂ SO ₄	5.1 µg h ⁻¹ cm ⁻²	7.1	-0.5	S37
WO ₃	0.5 M H ₂ SO ₄	4.2 µg h ⁻¹ mg ⁻¹ _{cat}	6.8	-0.12	14
CeO ₂ nanorod	0.1 M Na ₂ SO ₄	16.4 µg h ⁻¹ mg ⁻¹ _{cat}	3.7	-0.5	S38
β-FeOOH nanorods	0.5 M LiClO ₄	23.32 µg h ⁻¹ mg ⁻¹ _{cat}	6.7	-0.7	S39
MoS ₂ -rGO	0.1 M LiClO ₄	24.82 µg h ⁻¹ mg ⁻¹ _{cat}	4.58	-0.45	S40
DR MoS ₂ nanoflower	0.1 M Na ₂ SO ₄	29.28 µg h ⁻¹ mg ⁻¹ _{cat}	8.3	-0.4	15
MoS ₂	0.1 M Na ₂ SO ₄	8.08×10 ⁻¹¹ mol s ⁻¹ cm ⁻²	1.17	-0.5	16
Sn/SnS2	0.1 M NaOH	23.8 µg h ⁻¹ mg ⁻¹	6.5	-0.8	S41
Fe ₃ S ₄	0.1 M HCl	75.4 µg h ⁻¹ mg ⁻¹ _{cat}	6.45	-0.4	S42
CoS ₂	0.1 M HCl	17.45 µg h ⁻¹ mg ⁻¹ _{cat}	4.6	-0.15	S43
VN/CC	0.1 M HCl	2.48×10 ⁻¹⁰ mol s ⁻¹ cm ⁻²	3.58	-0.3	17
Fe ₁ -N-C	1 M NaClO	1.56×10 ⁻¹¹ mol s ⁻¹ cm ⁻²	4.51	-0.05	S44
Fe-N/C	0.1 M KOH	34.83 µg h ⁻¹ mg ⁻¹ _{cat}	9.28	-0.2	18
CSA/NPC	0.05 M Na ₂ SO ₄	0.86 µmol h ⁻¹ cm ⁻²	10.5	-0.2	S45
B Nanosheet	0.1 M Na ₂ SO ₄	13.22 µg h ⁻¹ mg ⁻¹ _{cat}	4.04	-0.80	19
B nanosheets	0.1 M HCl	3.12 µg h ⁻¹ mg ⁻¹ _{cat}	4.84	-0.14	S46
Defect Graphene	0.01 M H ₂ SO ₄	4.31 µg h ⁻¹ mg ⁻¹ _{cat}	8.51	-0.4	20
rGO	0.5 M LiClO ₄	17.02 µg h ⁻¹ mg ⁻¹ _{cat}	4.83	-0.75	S47

13. Computational methods

All electronic structure calculations were performed using the SIESTA package with Troullier-Martins norm conserving pseudopotentials.^{S48-S50} The exchange-correlation functional utilized was at the generalized gradient approximation (GGA) level with Perdew-Burke-Ernzerhof (PBE).^{S51} A double- ξ plus polarization (DZP) basis set was employed and the orbital-confirmed cutoff was determined from an energy shift of 0.01 eV. The Au(111), Au(110) and Au(310) slabs were modeled by a $p(3\times 3)$, $p(2\times 3)$, and $p(3\times 3)$ super cell with 36, 24 and 36 Pt atoms respectively, are shown in Fig. S9. The Monkhorst-Pack k -point mesh for describing the Brillouin zones was $4\times 4\times 1$ for Au(111), $6\times 4\times 1$ for Au(110) and $4\times 4\times 1$ for Au(310). The bottom half Au atoms were fixed at their bulk positions and other atoms with intermediates were allowed to move during optimizations. The cut-off energy for the real space grid was 250 Ry. The vacuum region was ~ 15 Å to eliminate interactions between slabs in the z direction.

The Gibbs free energy of species was obtained from $G = E + ZPE - TS$, where E is the total energy of species, S is the entropy and ZPE is the zero point energy at 300 K. The reaction free energy of $A + H^+ + e^- \rightarrow AH$ was calculated as $\Delta G = E(AH) - E(H^+ + e^-) - E(AH) + \Delta ZPE - T\Delta S$. At the electrode potential of 0 V, pH = 0 ($[H^+] = 1M$), at 298 K, due to the equilibrium of $H^+ + e^- \rightarrow \frac{1}{2} H_2$, we can use the free energy of $\frac{1}{2} H_2$ in the gas phase to replace that of $H^+ + e^-$.^{S52} All vibrational frequencies of adsorbates, $v_i(\text{Hz})$, were calculated based on the harmonic oscillators approximation.^{S53} The adsorption energy was defined as: $E_{ad} = E(\text{ad/surf}) - E(\text{ad})$.

$E(\text{surf})$, where $E(\text{ad/surf})$, $E(\text{ad})$, and $E(\text{surf})$ are the total energies of the adsorbate binding to surface, free adsorbate in vacuum and clean surface, respectively.

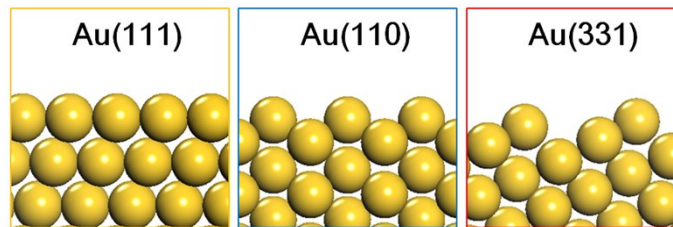


Fig. S13 Side views of theoretical models of Au(111), Au(110) and Au(331).

Table S3 Calculated reaction Gibbs free energies (unit in eV) of elementary steps for nitrogen reduction reactions including proton-electron transfer and N-N bond direct breaking steps under the electrode potential of -0.4 V (vs RHE) on Au(111), Au(110) and Au(331) respectively.

elementary steps	Au(111)	Au(110)	Au(331)
<i>proton-electron transfer processes</i>			
$\text{N}_2 + \text{H}^+ + \text{e}^- \rightarrow \text{N}_2\text{H}^*$	1.91	1.37	1.52
$\text{N}_2\text{H}^* + \text{H}^+ + \text{e}^- \rightarrow \text{N}_2\text{H}_2^*$	-0.92	-0.57	-0.68
$\text{N}_2\text{H}_2^* + \text{H}^+ + \text{e}^- \rightarrow \text{N}_2\text{H}_3^*$	-0.56	-0.85	-0.80
$\text{N}_2\text{H}_3^* + \text{H}^+ + \text{e}^- \rightarrow \text{N}_2\text{H}_4^*$	-1.14	-1.02	-1.13
$\text{N}_2\text{H}_3^* + \text{H}^+ + \text{e}^- \rightarrow \text{NH}^* + \text{NH}_3$	-0.76	-0.24	-0.75
$\text{N}_2\text{H}_4^* + \text{H}^+ + \text{e}^- \rightarrow \text{NH}_2^* + \text{NH}_3$	-1.07	-1.17	-1.07
$\text{NH}_2^* + \text{H}^+ + \text{e}^- \rightarrow \text{NH}_3$	-1.28	-0.82	-0.90
<i>N-N bond direct breaking processes</i>			
$\text{N}_2 \rightarrow 2\text{N}^*$	5.73	5.37	4.85
$\text{N}_2\text{H}^* \rightarrow \text{N}^* + \text{NH}^*$	2.53	2.94	2.11
$\text{N}_2\text{H}_2^* \rightarrow 2\text{NH}^*$	1.42	2.38	1.50
$\text{N}_2\text{H}_3^* \rightarrow \text{NH}^* + \text{NH}_2^*$	0.53	0.59	0.15
$\text{N}_2\text{H}_4^* \rightarrow 2\text{NH}_2^*$	0.21	-0.34	-0.18

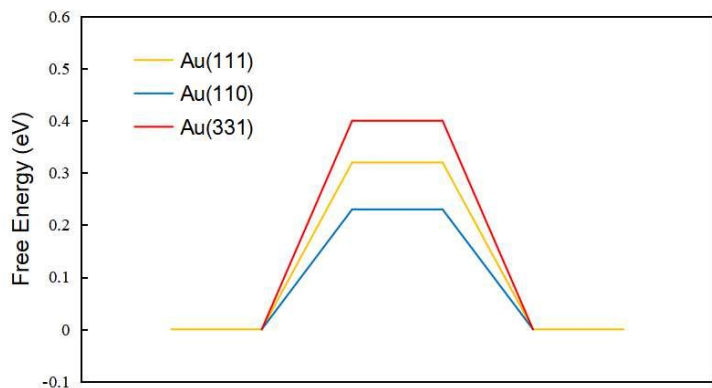


Fig. S14 Gibbs free energy profiles for hydrogen evolution reactions on Au(111), Au(110) and Au(331) under standard electrode potential.

References

- S1 L. Wei, Y.-J. Fan, H.-H. Wang, , N. Tian Z.-Y. Zhou, and S.-G. Sun, *Electrochim. Acta*, 2012, **76**, 468.
- S2 L. Wei, Y.-J. Fan, N. Tian, Z.-Y. Zhou, X.-Q. Zhao, B.-W. Mao, and Shi-Gang Sun, *J. Phys. Chem. C*, 2012, **116**, 2040.
- S3 L. Wei, Z.-Y. Zhou, S.-P. Chen, C.-D. Xu, D. Su, M. E. Schuster, and S.-G. Sun, *Chem. Commun.*, 2013, **49**, 11152.
- S4 H. Wang, H. Yu, Z. Wang, Y. Li, Y. Xu, X. Li, H. Xue, and L. Wang, *Small*, 2019, **15**, 1804769.
- S5 Q. Qin, T. Heil, M. Antonietti, and M. Oschatz, *Small Methods*, 2018, **2**, 1800202.
- S6 D. Liu, G. Zhang, Q. Ji, Y. Zhang and J. Li, *ACS Appl. Mater. Interfaces*, 2019, **11**, 25758.

- S7 L. Ji, X. Shi, A. M. Asiri, B. Zheng, and X. Sun, *Inorg. Chem.*, 2018, **57**, 14692.
- S8 W.-Y. Gao, Y.-C. Hao, X. Su, L.-W. Chen, T.-A. Bu, N. Zhang, Z.-L. Yu, Z. Zhu, and A.-X. Yin, *Chem. Commun.*, 2019, **55**, 10705.
- S9 D. Wang, L. M. Azofra, M. Harb, L. Cavallo, X. Zhang, B. H. R. Suryanto, and D. R. MacFarlane, *ChemSusChem*, 2018, **11**, 3416.
- S10 C. Li, S. Mou, X. Zhu, F. Wang, Y. Wang, Y. Qiao, X. Shi, Y. Luo, B. Zheng, Q. Li, and X. Sun, *Chem. Commun.*, 2019, **55**, 14474.
- S11 X. Guo, W. Yi, F. Qu, and L. Lu, *J. Power Sources*, 2020, **448**, 227417.
- S12 M. Nazemi, and M. A. El-Sayed, *J. Phys. Chem. C*, 2019, **123**, 11422-11427.
- S13 Y. Liu, L. Huang, X. Zhu, Y. Fang, and S. Dong, *Nanoscale*, 2020, **12**, 1811.
- S14 H. Wang, D. Yang, S. Liu, S. Yin, Y. Xu, X. Li, Z. Wang, and L. Wang, *ACS Sustainable Chem. Eng.*, 2019, **7**, 15772.
- S15 F. Pang, F. Wang, L. Yang, Z. Wang, and W. Zhang, *Chem. Commun.*, 2019, **55**, 10108.
- S16 F. Pang, Z. Wang, K. Zhang, J. He, W. Zhang, C. Guo, and Y. Ding, *Nano Energ.*, 2019, **58**, 834.
- S17 W. Fu, Y. Cao, Q. Feng, W. R. Smith, P. Dong, M. Ye, and J. Shen, *Nanoscale*, 2019, **11**, 1379.
- S18 H. Wang, Y. Li, C. Li, K. Deng, Z. Wang, Y. Xu, X. Li, H. Xue, and L. Wang, *J. Mater. Chem. A*, 2019, **7**, 801.
- S19 J. Bai, H. Huang, F.-M. Li, Y. Zhao, P. Chen, P.-J. Jin, S.-N. Li, H.-C. Yao, J.-H. Zeng, and Y. Chen, *J. Mater. Chem. A*, 2019, **7**, 21149.

- S20 C. Fang, T. Bi, X. Xu, N. Yu, Z. Cui, R. Jiang, and B. Geng, *Adv. Mater. Interfaces*, 2019, **6**, 1901034.
- S21 L. Yang, T. Wu, R. Zhang, H. Zhou, L. Xia, X. Shi, H. Zheng, Y. Zhang, and X. Sun, *Nanoscale*, 2019, **11**, 1555.
- S22 R. Zhang, H. Guo, L. Yang, Y. Wang, Z. Niu, H. Huang, H. Chen, L. Xia, *ChemElectroChem*, 2019, **6**, 1014.
- S23 L. Xia, B. Li, Y. Zhang, R. Zhang, L. Ji, H. Chen, G. Cui, H. Zheng, X. Sun, F. Xie, and Q. Liu, *Inorg. Chem.*, 2019, **58**, 2257.
- S24 X. Zheng, Z. Zhang, X. Li, and C. Ding, *New J. Chem.*, 2019, **43**, 7932.
- S25 H. Huang, F. Gong, Y. Wang, H. Wang, X. Wu, W. Lu, R. Zhao, H. Chen, X. Shi, A. M. Asiri, T. Li, Q. Liu, and X. Sun, *Nano Res.*, 2019, **12**, 1093.
- S26 X. Wu, L. Xia, Y. Wang, W. Lu, Q. Liu, X. Shi, and X. Sun, *Small*, 2018, **14**, 1803111.
- S27 Z. Wang, K. Zheng, S. Liu, Z. Dai, Y. Xu, X. Li, H. Wang, and L. Wang, *ACS Sustainable Chem. Eng.*, 2019, **7**, 11754.
- S28 X. Xiang, Z. Wang, X. Shi, M. Fan, and X. Sun, *ChemCatChem*, 2018, **10**, 4530.
- S29 Q. Liu, X. Zhang, B. Zhang, Y. Luo, G. Cui, F. Xie, and X. Sun, *Nanoscale*, 2018, **10**, 14386.
- S30 K. Chu, Y. Liu, Y. Li, H. Zhang, and Y. Tian, *J. Mater. Chem. A*, 2019, **7**, 4389.
- S31 X. Wang, J. Wang, Y. Li, and K. Chu, *ChemCatChem*, 2019, **11**, 4529.
- S32 K. Chu, Y. Liu, J. Wang, and H. Zhang, *ACS Appl. Energy Mater.*, 2019, **2**, 2288.
- S33 F. Wang, Y. Liu, H. Zhang, and K. Chu, *ChemCatChem*, 2019, **11**, 1441.

- S34 Y. Liu, Y. Li, D. Huang, H. Zhang, and K. Chu, *Chem. Eur. J.*, 2019, **25**, 11933.
- S35 X. Li, L. Li, X. Ren, D. Wu, Y. Zhang, H. Ma, X. Sun, B. Du, Q. Wei, and B. Li, *Ind. Eng. Chem. Res.*, 2018, **57**, 16622.
- S36 L. Huang, J. Wu, P. Han, A. M. Al-Enizi, T. M. Almutairi, L. Zhang, and G. Zheng, *Small Methods*, 2019, **3**, 1800386.
- S37 K. Chu, Y. Liu, Y. Li, J. Wang, and H. Zhang, *ACS Appl. Mater. Interfaces*, 2019, **11**, 31806.
- S38 B. Xu, L. Xia, F. Zhou, R. Zhao, H. Chen, T. Wang, Q. Zhou, Q. Liu, G. Cui, X. Xiong, F. Gong, and X. Sun, *ACS Sustainable Chem. Eng.*, 2019, **7**, 2889.
- S39 X. Zhu, Z. Liu, Q. Liu, Y. Luo, X. Shi, A. M. Asiri, Y. Wu, X. Sun, *Chem. Commun.*, 2018, **54**, 11332.
- S40 X. Li, X. Ren, X. Liu, J. Zhao, X. Sun, Y. Zhang, X. Kuang, T. Yan, Q. and Wei, D. Wu, *J. Mater. Chem. A*, 2019, **7**, 2524.
- S41 P. Li, W. Fu, P. Zhuang, Y. Cao, C. Tang, A. B. Watson, P. Dong, J.g Shen, and M. Ye, *Small*, 2019, **15**, 1902535.
- S42 X. Zhao, X. Lan, D. Yu, H. Fu, Z. Liu, and T. Mu, *Chem. Commun.*, 2018, **54**, 13010.
- S43 P. Wei, H. Xie, X. Zhu, R. Zhao, L. Ji, X. Tong, Y. Luo, G. Cui, Z. Wang, and X. Sun, *ACS Sustainable Chem. Eng.*, 2020, **8**, 29.
- S44 R. Zhang, L. Jiao, W. Yang, G. Wan, and H.-L. Jiang, *J. Mater. Chem. A*, 2019, **7**, 26371.
- S45 Y. Liu, Q. Xu, X. Fan, X. Quan, Y. Su, S. Chen, H. Yu, and Z. Cai, *J. Mater.*

Chem. A, 2019, **7**, 26358.

S46 Q. Fan, C. Choi, C. Yan, Y. Liu, J. Qiu, S. Hong, Y. Jung, and Z. Sun, *Chem. Commun.*, 2019, **55**, 4246.

S47 Y. Song, T. Wang, J. Sun, Z. Wang, Y. Luo, . Zhang, H. Ye, and X. Sun, *ACS Sustainable Chem. Eng.*, 2019, **7**, 14368.

S48 J. M. Soler, E. Artacho, J. D. Gale, A. Garcia, J. Junquera, P. Ordejon and D. Sanchez-Portal, *J. Phys.: Condens. Matter*, 2002, **14**, 2745.

S49 J. Junquera, O. Paz, D. Sanchez-Portal and E. Artacho, *Phys. Rev. B: Condens. Matter*, 2001, **64**, 235111.

S50 N. Troullier and J. L. Martins, *Phys. Rev. B: Condens. Matter*, 1991, **43**, 993.

S51 J. P. Perdew, K. Burke and M. Ernzerhof, *Phys. Rev. Lett.*, 1996, **77**, 386.

S52 J. K. Norskov, J. Rossmeisl, A. Logadottir, L. Lindqvist, J. R. Kitchin, T. Bligaard, and H. Jonsson, *J. Phys. Chem. B*, 2004, **108**, 17886.

S53 A. A. Gokhale, S. Kandoi, J. P. Greeley, M. Mavrikakis, and J. A. Dumesic, *Chem. Eng. Sci.*, 2004, **59**, 4679.